Vibration suppression of structures with viscoelastic inserts

ARTICLE *in* ARCHIVE PROCEEDINGS OF THE INSTITUTION OF MECHANICAL ENGINEERS PART C JOURNAL OF MECHANICAL ENGINEERING SCIENCE 1989-1996 (VOLS 203-210) · JANUARY 2002

Impact Factor: 0.56 · DOI: 10.1243/095440602760400959

3 AUTHORS, INCLUDING:

Bishakh Bhattacharya
Indian Institute of Technology Kanpur
62 PUBLICATIONS **150** CITATIONS

SEE PROFILE

Vibration suppression of structures with viscoelastic inserts

B Bhattacharya[1], **G R Tomlinson**[2*] and **J R House**[3]
[1]Mechanical Engineering Department, Indian Institute of Technology, Kanpur, India
[2]Department of Mechanical Engineering, University of Sheffield, UK
[3]QinetiQ, Farnborough, Hampshire, UK

Abstract: The concept of suppressing flexural and longitudinal wave motion in a free–free beam structure by use of embedded viscoelastic inserts is described. Taking the example of a simple aluminium beam it is shown that the shape of the insert in terms of the incident wave angle plays an important role in the efficient suppression of wave motion. The insert principle is then applied to a 'top-hat' stiffener section that forms part of a fibre-reinforced polymeric composite beam structure, typical of that used in the fabrication of marine structures. From this example it is shown that the use of specifically designed viscoelastic inserts can reduce flexural and longitudinal wave motion over a wide frequency range. The numerical studies are supported by experimental tests in the case of both the free–free beam and the more complex top-hat section structure.

Keywords: composite stiffener, viscoelastic damping, energy-absorbing joints, damped beams

NOTATION

a	viscoelastic insert width
b	width of the host beam
h	thickness of the viscoelastic insert
R	ratio of modal strain energies
U	strain energy
V	total volume of the viscoelastic insert
θ	insert angle (deg)
η	loss factor

1 INTRODUCTION

Viscoelastic damping materials are widely used for passive damping of vibration in marine, aerospace and surface-transport applications [**1–3**]. It is well known that the use of such materials in the junctions of a structure results in dissipation of vibrational energy of the structure due to the cyclic shear loading of the viscoelastic material [**4**].

The MS was received on 23 January 2002 and was accepted after revision for publication on 2 July 2002.
* *Corresponding author: Department of Mechanical Engineering, University of Sheffield, Mappin Street, Sheffield S1 3JD, UK.*

It has also been shown that by using such materials in the form of inserts in free–free beams, significant amounts of vibrational energy can be absorbed [**5**]. Early research by House [**6**] studied the viscoelastic insert principle with a specific view to suppressing longitudinal waves and further work by Bhattacharya *et al.* [**7**] studied the effect of inserts on longitudinal and flexural waves. Simple transmission line modelling and experimentation suggested that a tapered viscoelastic insert, embedded within the end of free–free fibre-reinforced polymer (FRP) composite beam, could dissipate longitudinal waves. Most effective dissipation was shown to occur when the mechanical impedance of the insert material was matched with that of the FRP material. This could be achieved by a bespoke combination of the dynamic mechanical properties and density of the viscoelastic insert polymer, its dimensions and geometry. More importantly it was found that tapering the insert material improved impedance matching, providing a gradual transition of the longitudinal waves into the insert polymer where the strain energy could then be dissipated. The rate of transition (i.e. the taper angle) was found to be important together with the overall length of the insert. However, this simplistic approach was inadequate to describe the taper angle and flexural wave effects on more complex structures such as those with added stiffeners, thus providing the requirement for the work described in this paper.

2 ANALYSIS OF FREE–FREE BEAMS WITH VISCOELASTIC INSERTS

In order to investigate the effect of shape on the effective damping, a simple beam model was used. Figure 1 shows a typical beam with a viscoelastic insert located at the centre. The total volume of the viscoelastic insert V is given by

$$V = \left[ah + \frac{h^2}{2}\cot\left(\frac{\theta}{2}\right)\right]b \tag{1}$$

where

a = width of the insert
h = thickness of the insert
b = width of the insert (and the beam)
θ = insert wedge angle

In order to analyse the effect of the wedge angle on the transverse and longitudinal waves, the volume of damping material V was kept constant while the width of the insert core a or thickness h may be varied to compensate for the effect of the change in θ. The concept is explained in Fig. 2. Apart from the variation in the geometric shape of the insert all the other properties of the beam were kept constant.

The core width of the insert a_i for any insert angle θ_1 may be expressed as

$$a_i = a_r + \frac{h}{2}\left[\cot\left(\frac{\theta_r}{2}\right) - \cot\left(\frac{\theta_i}{2}\right)\right], \quad i = 10, 20, \ldots, 150 \tag{2}$$

$$h_i = \frac{-a + \sqrt{a^2 + 4\alpha_1\alpha_2}}{2\alpha_1}, \quad i = 10, 20, \ldots, 150 \tag{3}$$

$$\alpha_1 = \frac{\cot(\theta_i/2)}{2}, \quad \alpha_2 = ah_r + \frac{h_r^2}{2}\cot\left(\frac{\theta_r}{2}\right) \tag{4}$$

2.1 Numerical studies

The beam and insert dimension geometry are shown in Fig. 3. The dynamic mechanical properties of the insert polymer were deliberately chosen for its damping behaviour at the frequencies and temperature of interest. Figure 4 illustrates the dynamic Young's modulus and associated loss factor with frequency at a temperature of 20 °C (i.e. that used for the experimental studies) for the insert material. For the host beam the Young's modulus was held constant at 70 GPa (base material, aluminium) and the damping of the beam material was assumed to be negligible. The modal loss factors were evaluated using the modal strain energy method [**8**]. The modal damping is estimated using a finite element (FE) model consisting of N elements using

$$\eta = \frac{\sum_{n=1}^{N} U_n\eta_n}{\sum_{n=1}^{N} U_n} \tag{5}$$

where η_n is the loss factor associated with the nth element, U_n is the strain energy of the nth element and η is the modal loss factor, the modal loss factor being

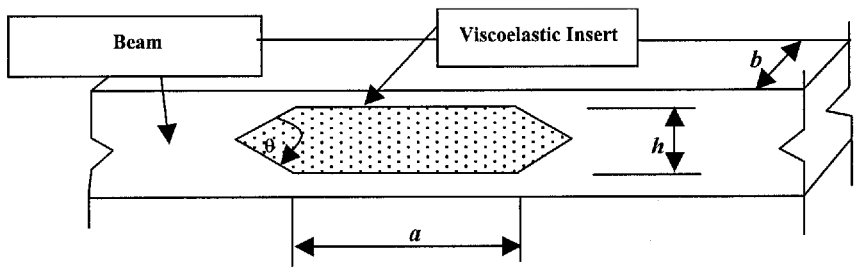

Fig. 1 A beam section with a viscoelastic insert. The insert extends through the width b of the beam

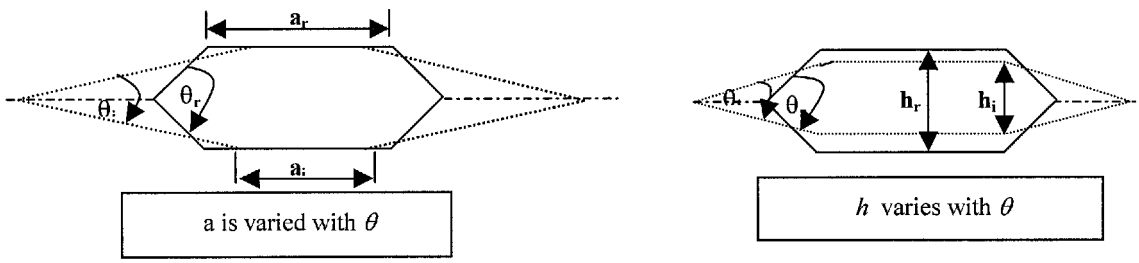

Fig. 2 Possible variation in the shape of the insert keeping the volume constant

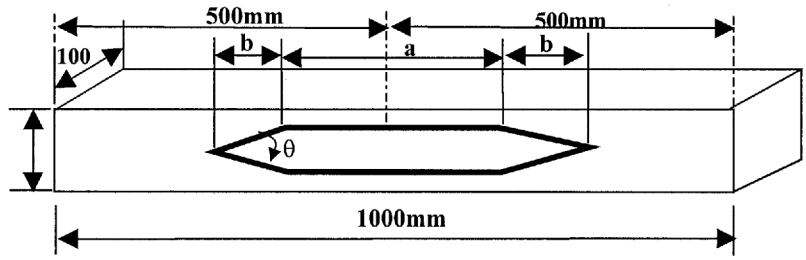

a	b	θ (deg)
32.33	67.66	25
63.78	36.21	45
74.01	25.98	60
85.00	15.00	90

Fig. 3 Beam and insert dimensions

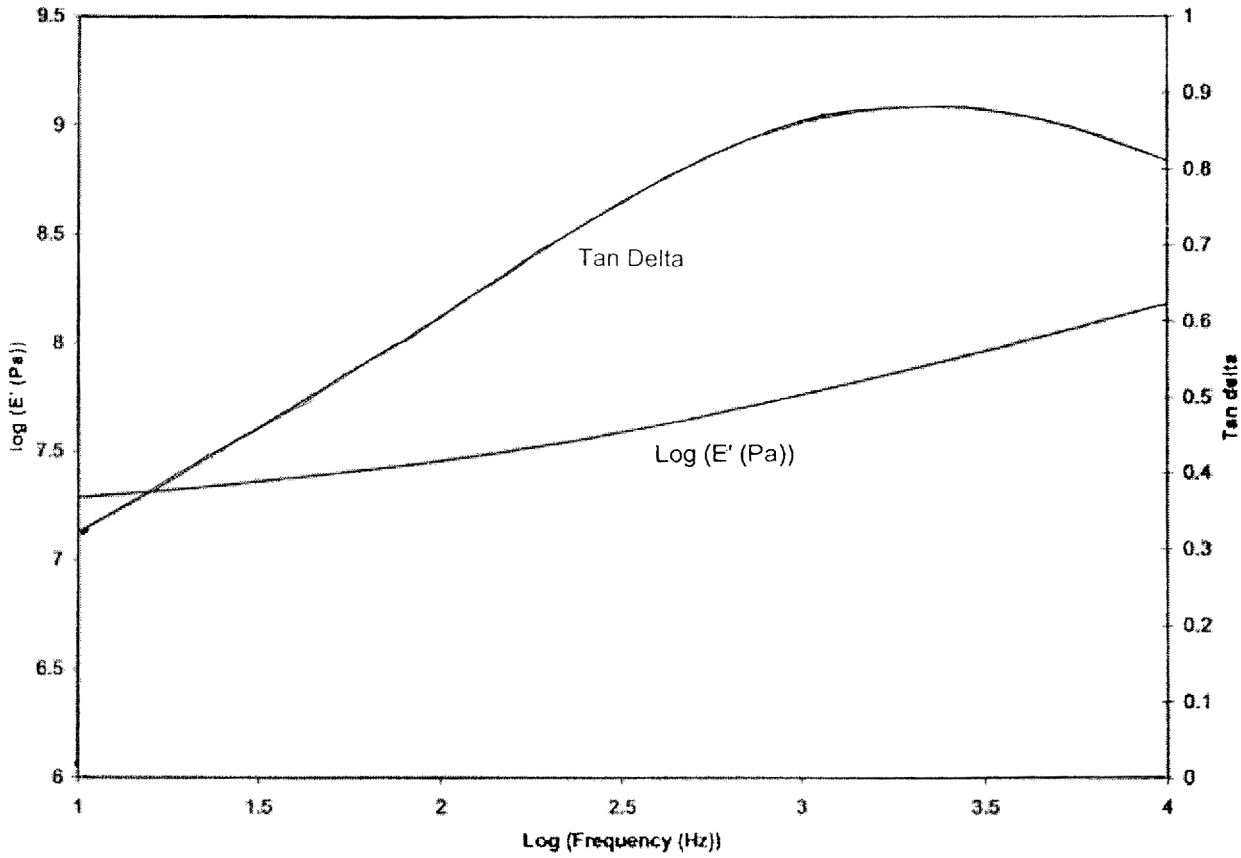

Fig. 4 Viscoelastic material properties at the operating temperature of 20 °C

defined as the loss factor of a vibration mode. The loss factor is the term used to describe the ratio of energy dissipated to energy stored during vibration and is a common measure of damping. It is used when hysteretic or viscoelastic damping predominates and, for low to moderate damping levels, is equivalent to twice the viscous damping measure zeta. In the case of structures where the loss factor of the host material is much less than that of the viscoelastic insert the above computation is simplified to

$$\eta = \eta_{\mathrm{v}} \frac{\sum_{i=1}^{P} U_i}{\sum_{n=1}^{N} U_n} = \eta_{\mathrm{v}} R \tag{6}$$

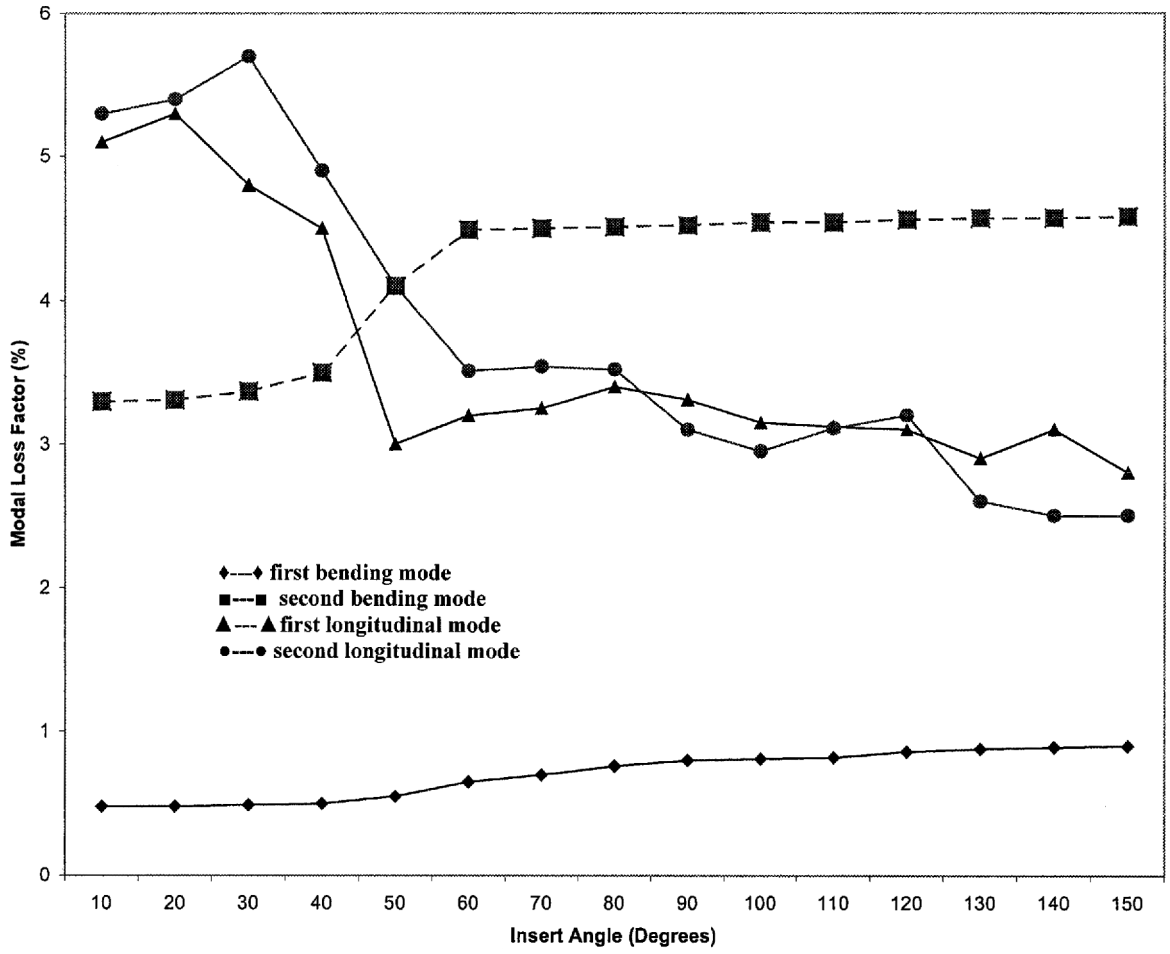

Fig. 5 Variation in the predicted modal loss factors with respect to the change in the insert angle

where R is the ratio of modal strain energies in the viscoelastic insert and the host structure respectively, U_i is the strain energy in the ith viscoelastic element and P is the number of viscoelastic elements.

The modal loss factors were computed for a range of insert angles from 10 to 150°. Beyond the insert angle of 150°, the wedge formed by the tapered section resulted in an ill-conditioning of elements during the FE modelling. A modal analysis using free–free boundary conditions was carried out up to a frequency range of 5 kHz. The first two bending and longitudinal modes were identified and chosen to estimate the trends in modal damping. The results are presented in Fig. 5.

In the case of the first and second bending modes, from about 10 to 40°, the modal loss factor remains almost insensitive to the increase in insert angle. From around 40–90°, there is an increase in the loss factor after which it remains almost constant. The loss factor is quite low for the first bending mode in comparison to the second mode, due to the placement of viscoelastic material at the geometric centre of the free–free beam. In the case of longitudinal modes, a reverse phenomenon has occurred, the loss factor is found to be high, from $\theta = 10°$ to 30°, for both first and second longitudinal modes. However, beyond this angle, it reduces until at approximately $\theta = 60°$ it remains relatively unchanged at a mean value of loss factor of about 3 per cent.

The variation of damping in the bending modes as the tapering of the wedge angle of the insert decreases is due to the variation of strain energy near the top and bottom through the depth of the beam. As the insert angle is reduced, the majority of the insert material becomes placed near the centre of the beam (i.e. the neutral plane of bending) where little or no strain can be imparted to the material. Thus it is not possible to provide effective dissipation of the vibrational energy. In the case of longitudinal waves, the strain is uniform along the cross-section; hence the location of the insert anywhere along the cross-section does not affect the damping performance. However, there is clearly a strong dependence of the modal loss factor on the insert angle as depicted in Fig. 5, particularly in the range 25–90° for both the bending and the longitudinal modes.

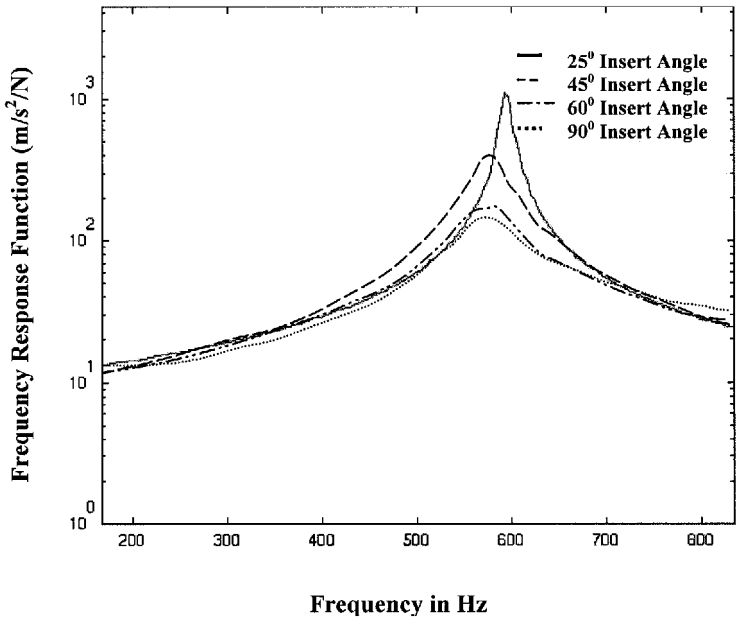

Fig. 6 Comparison of FRFs for the second bending mode

3 EXPERIMENTAL TESTING OF BEAMS WITH INSERTS

In order to carry out the experimental study, aluminium beams were fabricated corresponding to the properties shown in Fig. 3. The insert sizes were chosen based on the numerical analyses, which suggested the range of insert angles to be used for the study to be in the range 25–90°.

The beams were tested using free–free boundary conditions. For longitudinal excitation, the beams were suspended vertically whereas for transverse excitation they were suspended horizontally from the nodal points corresponding to the first bending mode. The beams were excited using random excitation in the frequency range 0–12 kHz. The modal loss factors were inferred from the measured frequency response functions. Typical measured frequency response functions for the second bending mode are shown in Fig. 6 for the four insert angles studied. The increase in the amount of damping can be clearly seen as the insert angle is increased.

The effect of insert angle on the measured modal damping in the first four modes is shown in Fig. 7. It is noted that the modal damping is quite low for the first bending mode (around 0.5 per cent). This is because of

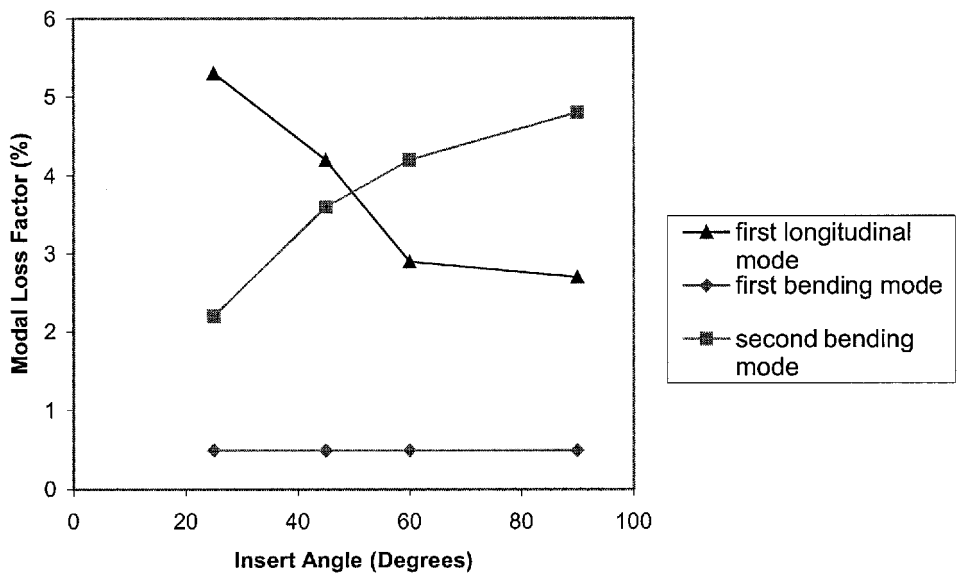

Fig. 7 Variation in the experimentally obtained modal loss factors with respect to the insert angle

Table 1 Comparison of predicted and measured modal loss factors

Mode	Predicted (%)	Measured (%)
First longitudinal (25°)	5.2	5.3
First bending (25°)	0.5	0.5
First longitudinal (45°)	3	4.1
First bending (45°)	0.55	0.5
First longitudinal (60°)	3	2.7
First bending (60°)	0.56	0.6
First longitudinal (90°)	3.2	2.8
First bending (90°)	0.75	0.75
Second bending (25°)	3.3	2.2
Second bending (45°)	4	3.75
Second bending (60°)	4.5	4.3
Second bending (90°)	4.5	4.4

the position of the insert. It is observed that, for the second bending mode, insert angles of 60 and 90° result in the highest damping, whereas, for the first longitudinal mode, the beam with a 25° insert angle has the highest damping. A comparison with the predicted data in Fig. 5 shows that the general trend is reflected in the measured data and comparison of the two is given in Table 1.

4 APPLICATION TO A COMPOSITE THS STRUCTURE

A 'top-hat' stiffener (THS) is a glass-reinforced polyester stiffened panel used in modern ship structures such as minesweepers. Figure 8a shows a traditional THS and Fig. 8b shows the THS with a viscoelastic insert. Table 2 gives details of the materials comprising the traditional THS and the THS with the viscoelastic insert.

An FE study on a section of the THS structure comprising one stiffener was carried out to assess the significance of the insert angle. Figure 9 shows the predicted modal strain energy ratio as a function of the insert angle. It is clear that an insert angle of around 30° offers a good compromise for damping both the flexural and the longitudinal waves.

A numerical modal analysis of the THS structure, with free–free boundary conditions over the frequency range 0–1 kHz was carried out using ABAQUS. The length of the structure was 3 m with three stiffeners at a centre spacing of 1 m and a width of 1 m. A schematic of this is shown in Fig. 10. The total number of nodes used for the analysis was 3309 and the total number of elements was 528. Twenty noded quadratic brick elements were chosen to model the geometry. For the composite body, C3D20 elements with nine integration points were chosen, while for the viscoelastic part, to reduce the possibility of computing spurious modes, C3D20R elements having a reduced integration in only four points were used.

An experimental modal test of the THS structure was also carried out using the configuration shown in Fig. 11. A band-limited excitation in the range 0–1 kHz was used to excite the structure in the longitudinal and flexural directions. The frequency response functions were measured using a DIFA data acquisition system operated by LMS software.

4.1 Modal analysis results

A comparison of the FE and experimental resonant frequencies for the traditional THS is shown in Fig. 12 for the first 24 resonant frequencies. A similar comparison for the THS with the viscoelastic insert was carried out and is shown in Fig. 13. The FE modal analysis could only be performed up to a frequency range of about 700 Hz. Beyond this range, the subspace iteration routine used by ABAQUS failed to converge, thereby limiting the modal analysis. However, the results obtained for the first 17 modes show good correlation.

The predicted (FE) and experimentally evaluated modal damping values for the traditional THS and the THS with viscoelastic inserts are plotted in Figs 14 and 15 respectively. The predicted and measured damping results are considered to correlate well. Modal damping estimated by FE analysis for the THS with the viscoelastic insert is between 1.3 and 3 per cent, whereas the experimental analysis has shown damping in the range 1.3–4 per cent. The presence of local modes may have affected the experimental results more than the numerically modelled results. In general, the THS with the viscoelastic inserts has resulted in a factor of about 3–4 increase in the modal damping in comparison with the traditional THS beam.

4.2 Transmissibility results

In order to assess the damping performance of the THS structure when subjected to longitudinal and transverse excitation, a series of transmissibility tests across the stiffeners was carried out over the frequency range 0–12 kHz for both the traditional THS and the THS with viscoelastic inserts. The transmissibility was measured at joints 1 to 3 (mid-way between the stiffeners) with respect to the excitation point at the 'near end', as indicated in Fig. 11.

Figure 16 shows the transmissibility results for the flexural response measured on the traditional THS structure. It can be seen that for the traditional THS there are no significant benefits regardless of the measurement station (i.e. joints 1 to 3). However, for the THS with the viscoelastic inserts (Fig. 17), the transmissibility reduces significantly when moving from joint 1 to joint 3, demonstrating the high damping efficiency of the inserts.

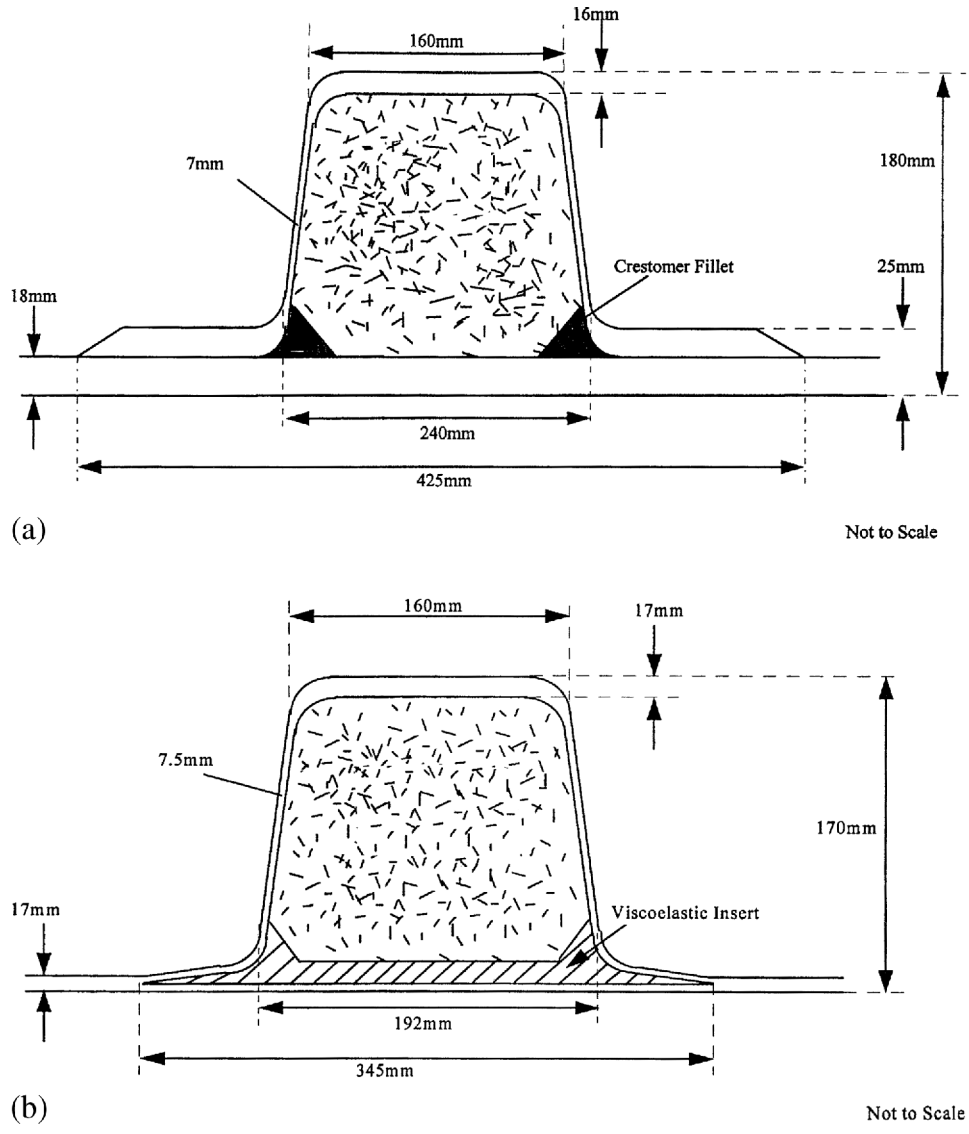

Fig. 8 Dimensions of (a) the traditional top-hat stiffener and (b) the top-hat stiffener with a viscoelastic insert

Table 2 Material properties of different subsections of the top-hat stiffener

	Property	Value
GRP laminate base plate	Modulus of elasticity	17 GPa
	Density	1600 kg/m^3
	Poisson's ratio	0.15
Side ply of the stiffener	Modulus of elasticity	17 GPa
	Density	1600 kg/m^3
	Poisson's ratio	0.110
Top ply of the stiffener	Modulus of elasticity	47 GPa
	Density	2000 kg/m^3
	Poisson's ratio	(0.31)
Viscoelastic insert	Modulus of elasticity	19 MPa
	Density	1600 kg/m^3
	Poisson's ratio	0.499
Crestomer fillet	Modulus of elasticity	1.5 GPa
	Density	1030 kg/m^3
	Poisson's ratio	0.350
Core material	Modulus of elasticity	6.0 GPa
	Density	200 kg/m^3
	Poisson's ratio	0.11

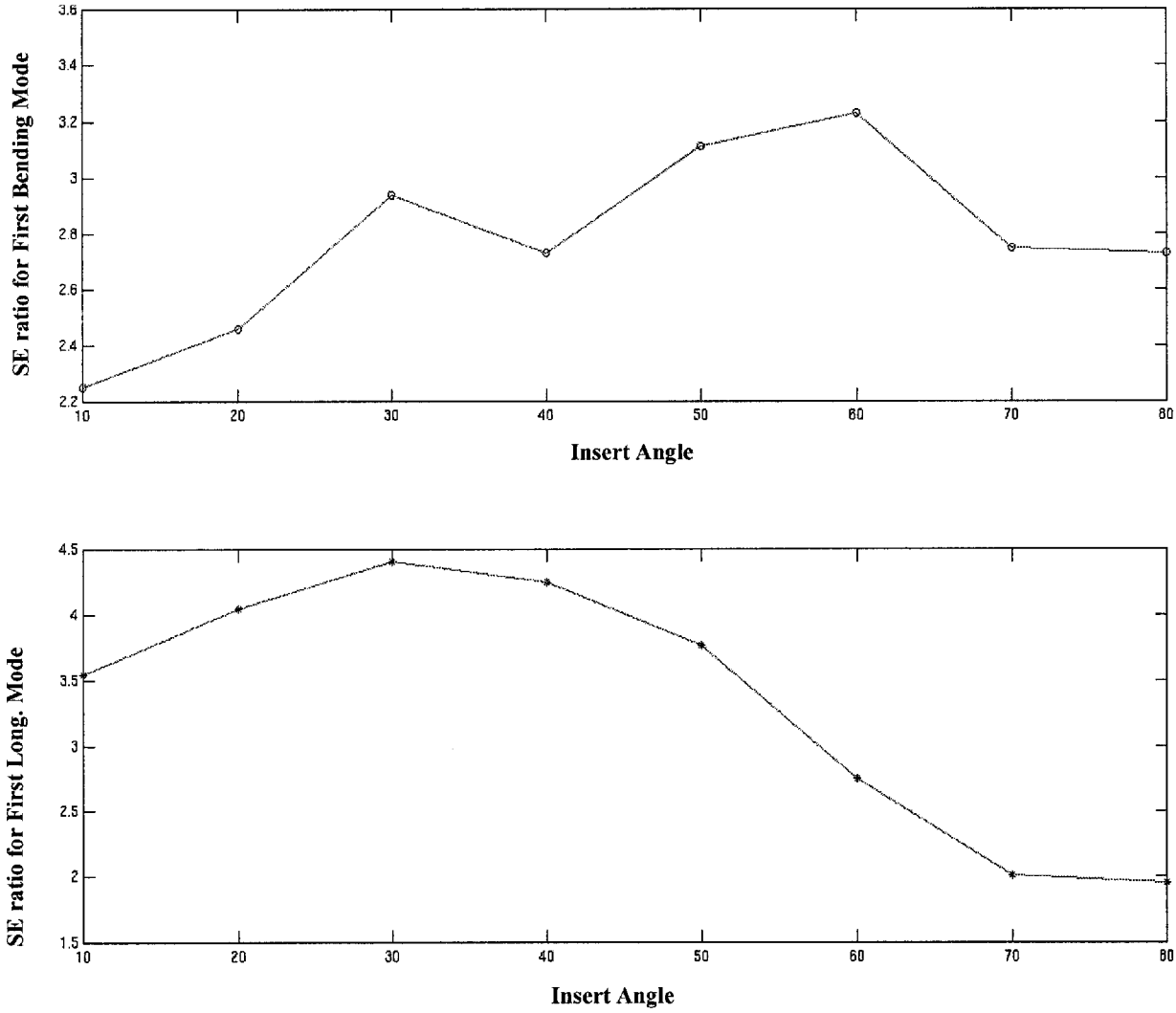

Fig. 9 Variation of the modal strain energy ratio for the top-hat stiffener with a change in the insert angle

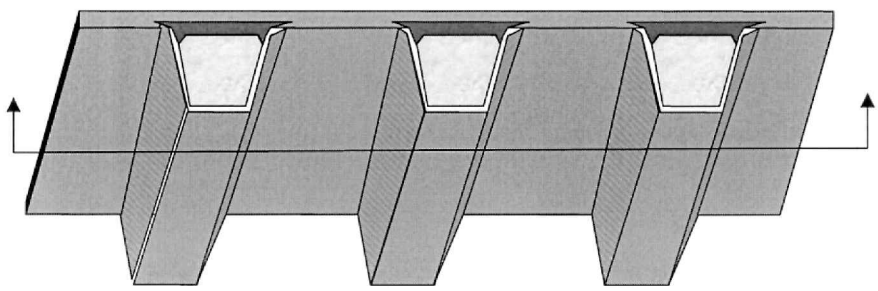

Fig. 10 Structural panel with a composite top-hat stiffener

In Figs 18 and 19 the longitudinal transmissibility results are shown. Only the direct response and the joint 3 transmissibility results are plotted. As shown in Fig. 19, significant improvement in longitudinal wave suppression is observed with the viscoelastic inserts as compared to the traditional THS structure.

5 CONCLUSIONS

The study into the shape of a viscoelastic insert for suppressing flexural and longitudinal waves using simple free–free beams has shown that there is a strong dependency on the incident wave angle of the insert.

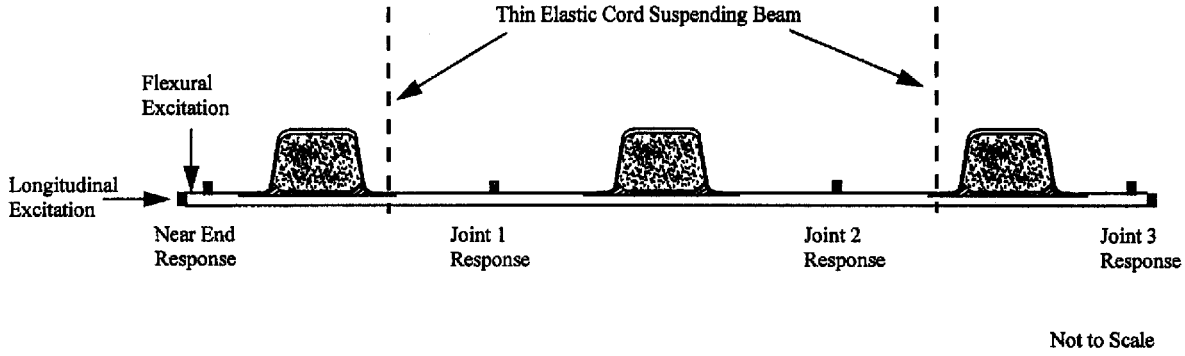

Fig. 11 Location of the point of excitation and measurement accelerometers

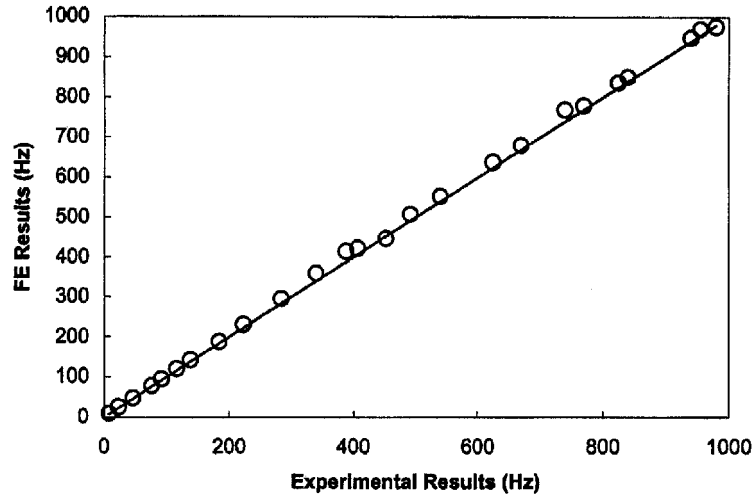

Fig. 12 Comparison of the FE and experimentally evaluated resonant frequencies of the traditional top-hat stiffener

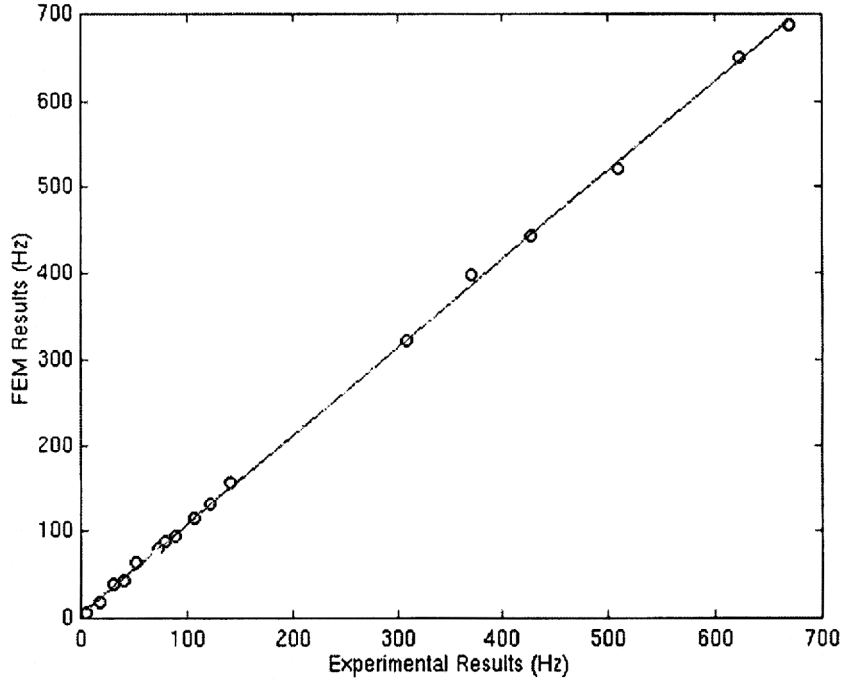

Fig. 13 Comparison of the FE and experimentally evaluated resonant frequencies of the top-hat stiffener with viscoelastic inserts

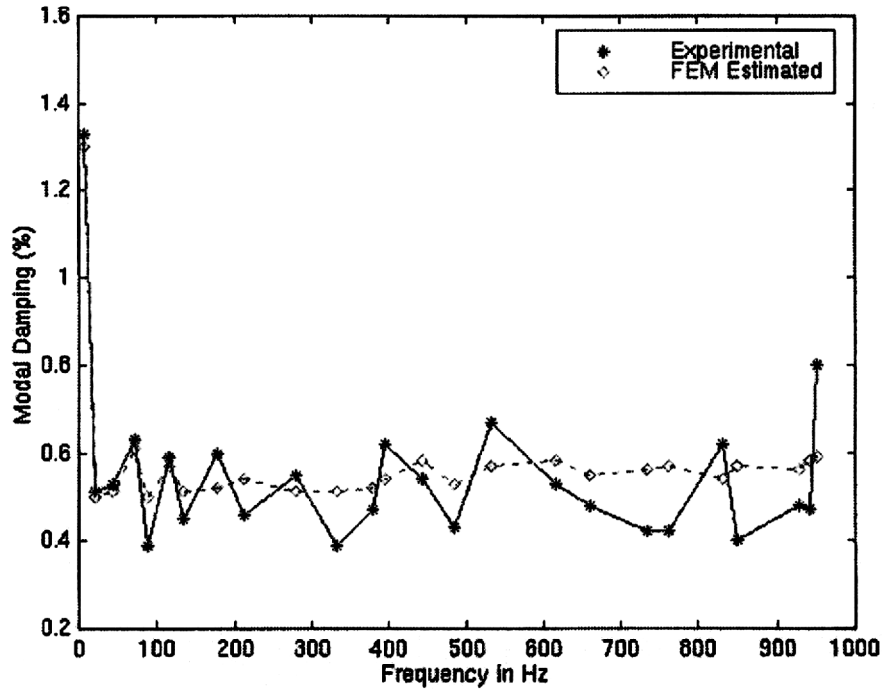

Fig. 14 Comparison of the FE and experimentally evaluated modal damping of the top-hat stiffener with traditional damping material

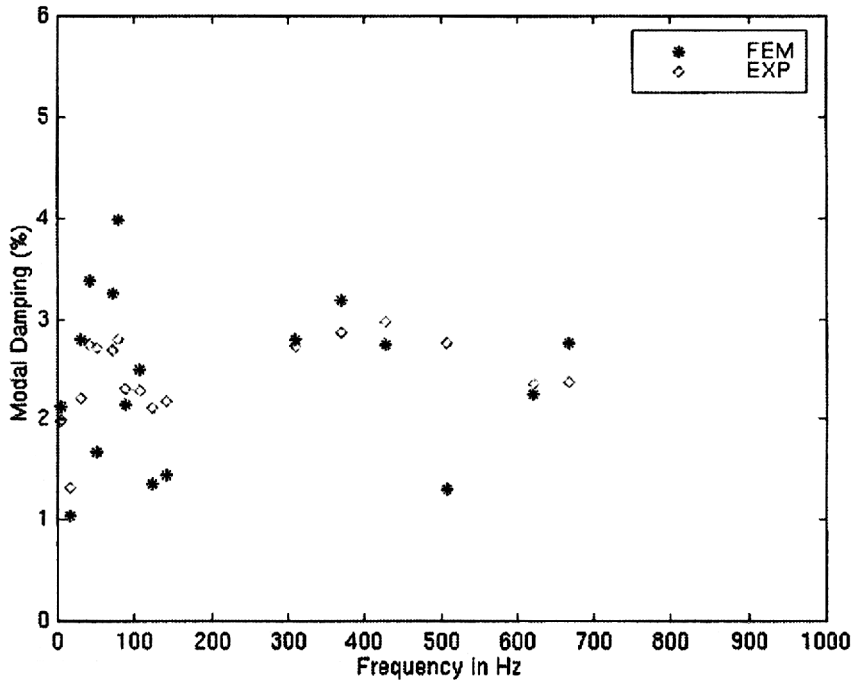

Fig. 15 Comparison of the FE and experimentally evaluated modal damping of the top-hat stiffener with a viscoelastic insert

When using viscoelastic materials, the level of damping achieved will be dependent on the dynamic mechanical properties and no attempt was made to optimize these at this stage or indeed to change the overall shape of the insert. The actual shape used in the top-hat section was based on earlier research where longitudinal waves were of prime consideration, but a different overall shape may well produce different results. However, what is very clear is that a localized use of a viscoelastic polymeric insert can provide significant dissipation of both longitudinal and flexural waves and that careful control of the incident wave angle has important

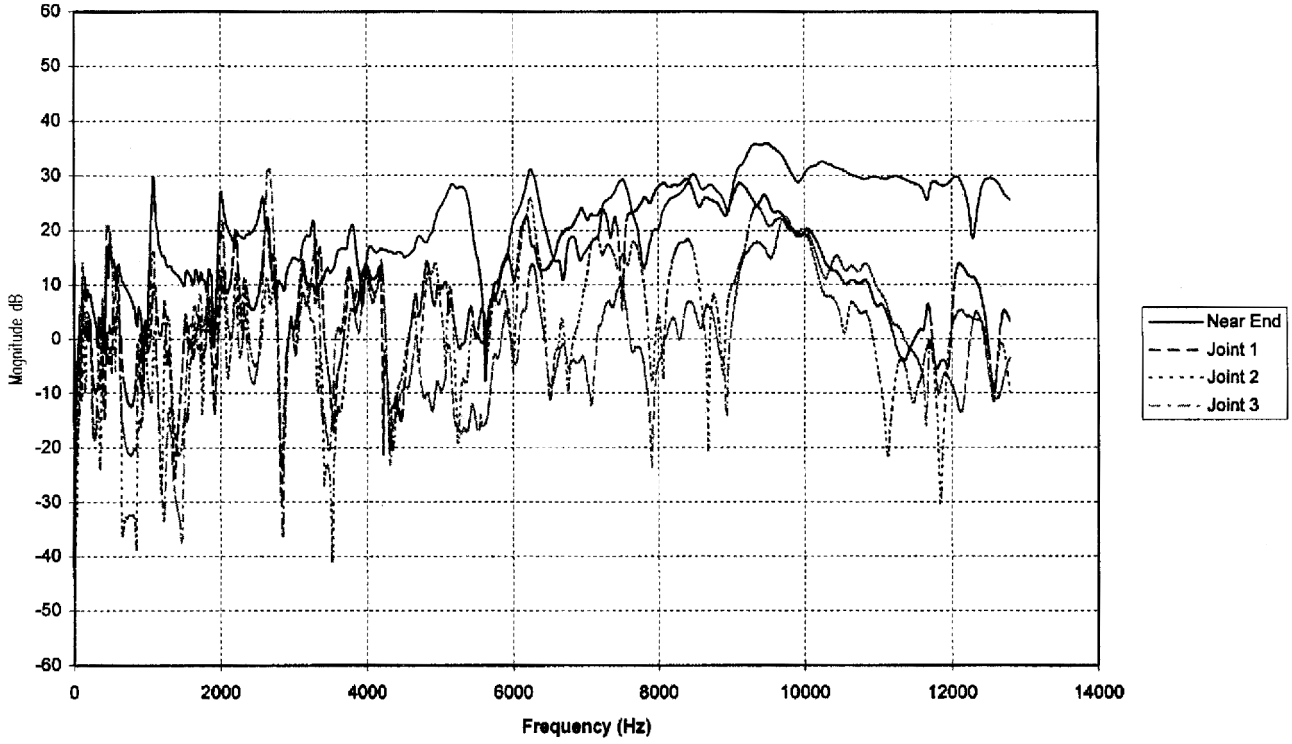

Fig. 16 Flexural response of a traditional top-hat stiffened beam

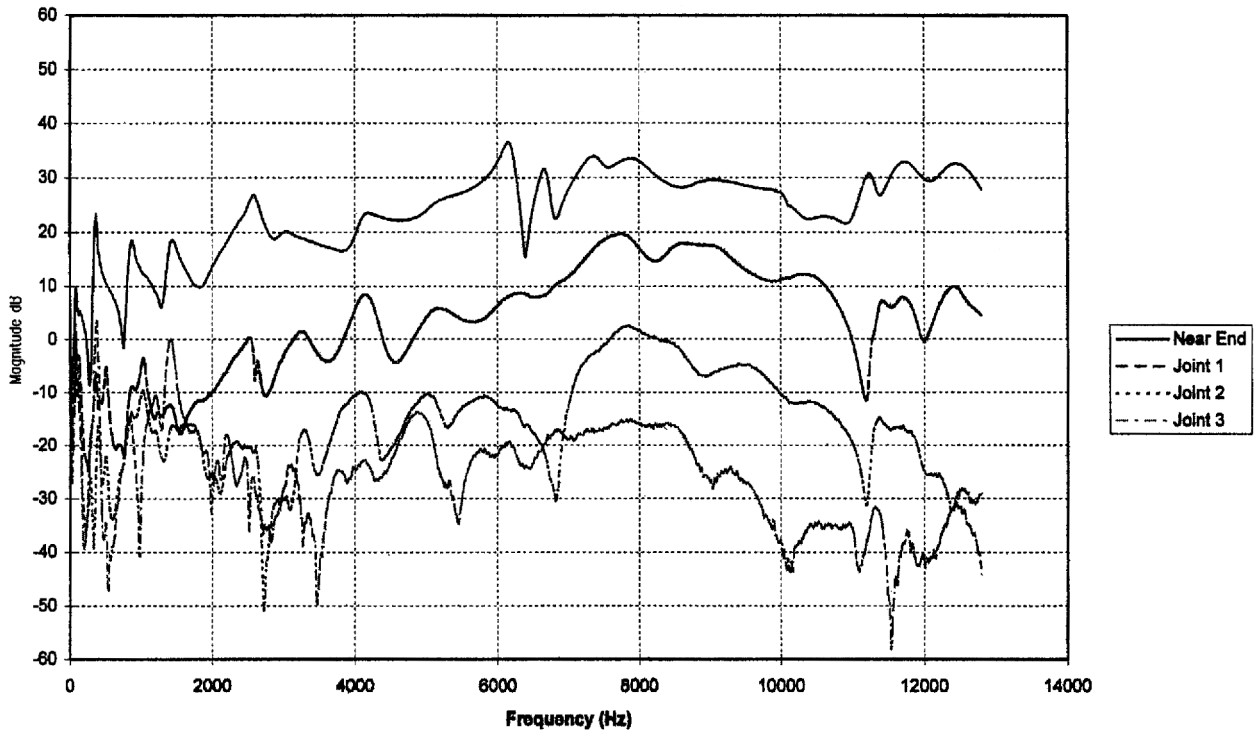

Fig. 17 Flexural response of a top-hat stiffened beam with viscoelastic inserts

implications for the levels of achievable structural damping. More research is required to fully understand the damping implications for variations in the length of the polymer insert, particularly for flexural waves. These results indicate that the use of such inserts in the fabrication of composite marine structures could be recommended where noise and vibration is an issue. The application to a THS composite structure revealed that

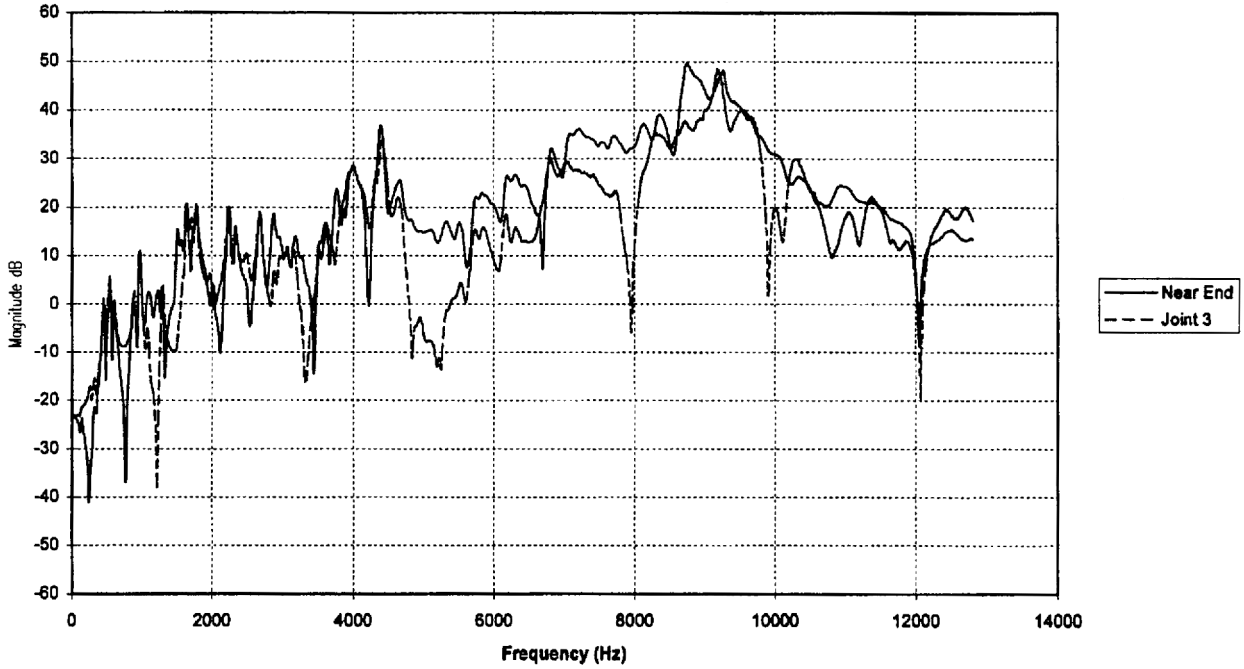

Fig. 18 Longitudinal response of a traditional top-hat stiffened beam

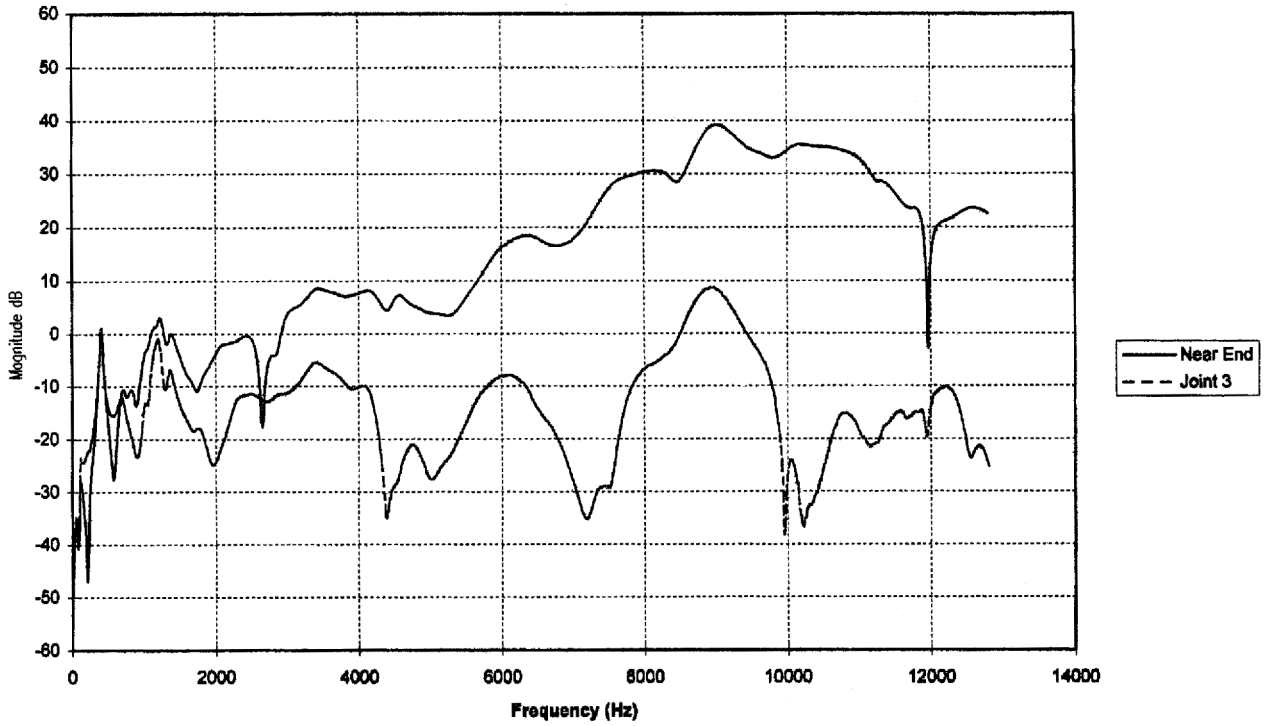

Fig. 19 Longitudinal response of a top-hat stiffened beam with viscoelastic inserts

significant levels of damping were achieved for both types of waves and that up to a 50 dB reduction in the flexural transmissibility across a 3 m span of the THS structure was possible across a frequency range spanning 0–12 kHz, with a viscoelastic insert having an incident wave angle of 30°.

REFERENCES

1 **Ferry, J. D.** *Viscoelastic Properties of Polymers*, 3rd edition, 1980 (John Wiley, New York).
2 **Ahid, N. D., Jones, I. G. D.** and **Henderson, J. P.** *Vibration Damping*, 1985 (John Wiley, New York).

3 Mallik, A. K. *Principles of Vibration Control*, 1st edition, 1990 (East-West Press).

4 Mentel, T. J. (Ed.) *Structural Damping*, 1960 (Pergamon Press, Oxford).

5 Bhattacharya, B., House, J. R. and **Tomlinson, G. R.** Low and high frequency energy absorbing composite joints. In SPIE 7th International Symposium on *Smart Structures and Materials*, Newport Beach, California, March 2000.

6 House, J. R. Observations on the use of a viscoelastic joint to provide noise reduced sonar domes. *Smart Mater. Structs*, 1997, **6**, 640–645.

7 Bhattacharya, B., House, J. R., Mercy, S. E. and **Tomlinson, G. R.** Finite element modeling and performance estimation of energy absorbing composite joints. In SPIE 6th Annual International Symposium on *Smart Structures and Materials*, March 1999.

8 Johnson, C. D. and **Kienholz, D. A.** Finite element prediction of damping in structures with constrained viscoelastic layers. *Am. Inst. Aeronaut. Astronaut. J.*, September 1982.